Applied Thermal Engineering 159 (2019) 113819

Contents lists available at ScienceDirect

Applied Thermal Engineering

journal homepage: www.elsevier.com/locate/apthermeng

Research Paper

A comparison of mixed convective heat transfer performance of nanofluids cooled heat sink with circular perforated pin fin

Fatima Zohra Bakhti[a], Mohamed Si-Ameur[b]

[a] University Med Boudiaf of M'sila, Faculty of Technology, Mechanical Department, 28000 M'sila, Algeria
[b] University of Batna 2, Faculty of Technology, Mechanical Department, LESEI/Avenue Chahid Boukhlouf Med Elhadi, 05000 Batna, Algeria

HIGHLIGHTS

- The heat sink with nanofluid undergoes the highest friction factor and pumping power compared to that of pure water.
- All the nanofluids used offer a more interesting heat transfer than in the case of the base fluid.
- The Nusselt number for "Cu + H_2O" is better than for "Al_2O_3 + H_2O" and "TiO_2 + H_2O".
- The Nusselt number decreases with the increase in the volumetric fraction of nanoparticles.

ARTICLE INFO

Keywords:
Nanofluids
Mixed convection
Heat sinks
Perforated pin fin
Finite volume method
Computational fluid dynamic

ABSTRACT

This paper presents a numerical study on the mixed convection of nanofluids in heat sinks with perforated circular fins. Four different types of nanofluids are used as cooling fluids, which are TiO_2, Al_2O_3 and Cu dispersed in pure water as the base fluid. The selected volumetric concentration of nanofluids was chosen in the range (2–10)%. The Reynolds number has changed in the range of 100–400 to ensure that flow remains in the laminar regime and to have the Richardson number $1 \leq Ri \leq 22$. To study the cooling performance of the heat sink, three-dimensional steady Navier Stokes and energy equations were discretized by the finite volume method using the power-law scheme and have been solved iteratively, using the SIMPLE algorithm. The results show that a significant improvement in heat transfer in the heat sink due to the suspension of nanoparticles in the base fluid compared to pure water, the improvement in heat transfer is intensified with increased Reynolds number and decrease in the volume fraction of nanoparticles. We also found that the low values of the average Nusselt number are obtained for the nanofluid TiO_2, the average values for Al_2O_3 and the highest values for Cu. It is important to note that a slight increase in friction factor and pumping power has been reported when nanofluid is used in the system.

1. Introduction

The study of cooling processes is of great interest, especially in the electronics industry where excessive heat production can cause damage and loss of equipment or electronics used. Improving convective transfer in cooling devices is equivalent to increasing heat exchange between a coolant and a hot surface.

All heat transfer intensification techniques will influence these two parameters: the convective heat exchange coefficient and the fluid/wall exchange surface. The addition of the fins acts mainly on the heat exchange surface, while the conductivity of the heat transfer fluid acts on the heat exchange coefficient.

Different techniques have been adopted to increase the efficiency of a cooling system. The first is that it is widely used to graft solid or perforated fins of different shapes [1–5] offering greater surface contact with the environment. The use of large surfaces such as fins is a reliable, economical and widely used method of heat dissipation.

Cooling large, high-powered systems requires greater heat dissipation. The second solution for heat removal is to use both the flow properties of liquids and the high thermal conductivity of solid metals. The use of nanofluids based on metal particles has a better thermal conductivity and a better convective heat transfer coefficient than the base fluid. This technique is certainly the most promising solution in the field of improving thermal transfer.

The use of ultrafine solid particles for dispersion in a base fluid was first introduced in 1993 by Masuda et al. [6]. Later, in 1995, Choi [7] first introduced the term "nanofluid", which conventionally means a fluid with a suspension of nanoparticles. Many researchers have stated

E-mail addresses: fatimazohra.bakhti@univ-msila.dz (F.Z. Bakhti), mohamed.siameur@univ-batna2.dz (M. Si-Ameur).

https://doi.org/10.1016/j.applthermaleng.2019.113819
Received 29 January 2019; Received in revised form 21 April 2019; Accepted 24 May 2019
Available online 25 May 2019
1359-4311/

Nomenclature

A	surface area for heat transfer
c_p	specific heat at constant pressure
d	pin fin diameter
D_h	hydraulic diameter
dt	pin fin perforation diameter
e_b	thickness of the base
e_s	thickness of electronic silicon component
f	friction factor
g	acceleration due to gravity
h	heat transfer coefficient
H_a	height of pin fin
H_t	height of the perforation of the pin fin
k_f	thermal conductivity of the fluid
k_{nf}	thermal conductivity of the nanofluid
k_S	heat sink thermal conductivity
$\dot{m}$	mass flow rate
Nu	Nusselt number based on D_h ($=h.D_h/K_f$)
PP	pumping power
Q	heat generated by the electronics component
qc	the heat convective flux
q_s	heat generated per unit volume
Re	Reynolds number
Ri	Richardson number
T_m	the bulk mean temperature
T_o	inlet fluid temperature
T_{out}	outlet fluid temperature
T_W	wall temperature of the heat sink
u, v, w	velocity components
u_0	inlet fluid velocity
x, y, z	Cartesian coordinates

Greek symbols

β	thermal expansion coefficient
ρ	the fluid density
μ	dynamic viscosity
φ	volumetric concentration

that replacing a coolant with a nanofluid improves the thermal performance of a base fluid [8–15]. Indeed, most solids have a higher thermal conductivity than the thermal conductivity of the base fluid. Thus, the addition of nanoparticles to the base fluid has created higher thermal conductivity values and improved thermal performance compared to the base fluid.

The design of the optimal heat sink configuration combined with a nanofluid as coolant can be the optimal solution for efficient heat dissipation of the modern electronic system. Several research studies on heat transfer have been carried out in recent decades to develop new techniques to improve transfer performance by using metallic additives to base fluids to increase their thermal conductivity used in cooling finned heat sinks of different shapes.

Jang and Choi [16] discovered that the use of diamond -water nanofluid as a coolant for a micro-channel heat sink improves thermal performance by about 10% compared to distilled water.

Li and Kleinstreuer [17], Seyed et al. [18], Ghazvini and Shokouhmand [19], Selvakumar and Suresh [20] examined the thermal performance of CuO nanoparticles dispersed in water. The assembly is a nanofluid used in the cooling of trapezoidal, rectangular and circular finned heat exchangers. The results indicate that the addition of nanoparticles to the water leads to an improvement in the thermal performance of the heat sink with a slight increase in pumping power. They also found that the nanofluid CuO-water has a significant effect on reducing the temperature of the heat sink base compared to distilled water.

Mohammed et al. [21], Ho et al. [22], Kalteh et al. [23], HO and Chen [24], Anbumeenakshi and Thansekhar [25], Sohel et al. [26], Ho et al. [27], Seyed et al. [28] and Muhammad Saeed and Man-Hoe Kim [29] conducted numerical and experimental studies on the flow characteristics and heat transfer of the nanofluid Al_2O_3-water in a microchannel thermal heat sink. The results showed a significant increase in the thermal transfer coefficient, for different increasing values of volume fractions with a significant reduction in thermal resistance.

Mohammed et al. [30] analyzed the influence of the use of different types of nanofluids on heat transfer and fluid flow characteristics in a triangular microchannel heat sink. The nanofluids used are Al_2O_3, Ag, CuO, Diamond, SiO_2 and TiO_2, all with water as the base fluid. They noted that the nanofluid Diamond-H_2O has the lowest temperature and the highest thermal transfer coefficient. While the Ag-H_2O has the lowest pressure drop and shear stress of the wall. Therefore, Diamond-H_2O and Ag-H_2O nanofluids are recommended to improve overall heat transfer and reduce pressure drop compared to pure water.

Hung et al. [31] studied the improvement of the thermal performance of a rectangular microchannel heat sink using different nanoparticles (Al_2O_3, CuO, TiO_2, Cu, Ag and diamond) dispersed in water and other base fluids (Al_2O_3 - ethylene glycol (EG) and Al_2O_3 - motor oil (EO)). The results showed that the increase in the convective transfer coefficient is greater for the nanofluids Al_2O_3-water and diamond-water than for the other types of nanofluids used. They also noted that the base fluids with low dynamic viscosity such as water have better thermal performance than base fluidswith a higher dynamic viscosity such as engine oil.

Ijam and Saidur [32,33] presented a numerical study of the flow and heat transfer characteristics of minichannel heat sinks operating with nanofluids TiO_2-water, Al_2O_3-water and SiC-water at particle volume fractions of 0.8%, 1.6%, 2.4%, 3.2% and 4.0%. They report that cooling has been improved by 17.3% and 16.5% using Al_2O_3 and TiO_2 nanoparticles respectively.

Manay et al. [34] and Albdoor [35] have successfully used Al_2O_3-water and Cu-water as coolant to improve the thermal performance of a microchannel heat sink. Their results showed that Cu water has a better thermal performance than Al_2O_3 water.

Tokit et al. [36] numerically presented the thermal performance of an interrupted microchannel heat sink using Al_2O_3-water, CuO-water and SiO_2-water nanofluids with particle fractions between 1% and 4%.

Hashemi et al. [37] quantified the thermal performance of the nanofluid SiO_2-watercooled miniature flat plate heat sink with particle volume fractions of 3.5%, 4.0%, 4.5%, 4.5%, 4.5%, 5% and 5.0% in a laminar flow regime.

Naphon and Nakharintr [38] studied the thermal transfer characteristics of nanofluids in a mini rectangular heat sink. The nanofluid used is TiO_2 water. They found that the average heat transfer rates for nanofluids are higher than those for pure water.

Mushtaq Ismael Hasan [39] numerically studied the thermal performance of a heat sink with three fin geometries (square, triangular and circular) and two types of nanofluids (Diamond-water and Al_2O_3-water) used as coolant, in addition to pure water. The volumetric concentration of the selected nanofluids was chosen from the range (1–4)%. The results obtained indicate that the use of a nanofluid instead of pure water as a refrigerant improves thermal performance by increasing the amount of heat dissipated, but also results in an increased pressure drop for all forms and nanofluids studied.

Abudakar and Sidi [40,41] used Fe_2O_4- water as a coolant in a numerical study of heat transfer and laminar flow in a microchannel heat sink. A significant improvement in heat transfer was observed with

the increase in the volume fraction of nanoparticles

Zhang et al. [42] and Arshad and Ali [43] conducted an experimental study to investigate the effect of nanofluids on the thermal and hydraulic performance of a mini-channel heat sink. They showed that the use of the nanofluid TiO_2-H_2O increased the heat transfer coefficient and pressure drop.

Many of the literature researches have been conducted to study heat transfer and flow characteristics in full pine fin heat sink with different nanofluids, and the little research that has studied the cooling of perforated fins and the improvement made by increasing the heat exchange surface by adding perforations to the fins.

Therefore, the objective of this paper is to study numerically mixed convection heat transfer in a new design of circular perforated finned heat sink using different nanoparticles of TiO_2, Al_2O_3 and Cu dispersed in the water base fluid under laminar flow. In addition, the CFD model is simulated by a finite volume method and using FLUENT software to solve the governing equations. The Reynolds number is between 100 and 400, the Richardson number is $1 \leq Ri \leq 22$ and the volume fraction of the nanofluid is 2 to 10%. The strategy adopted follows the earlier works Salhi et al. [44], Bakhti and Si-Ameur [5] of the authors of this article. The objective of this work is to study the improvement of heat transfer convection in terms of Nusselt number by proposing this new fin design and using nanofluids as a coolant.

2. Mathematical modeling

2.1. Geometrical configuration

The geometry of the problem studied is shown schematically in Fig. 1, it is an aluminium heat sink with 17 perforated cylindrical perforated fins of diameter d = 1 cm and height Ha = 5 cm. The fins are fixed in staggered arrangement to a parallelepipedic base measuring 8 cm × 6 cm and having a thickness e_b = 1 cm. The bottom of the heat sink is mounted on a silicon electronic component with a thickness of e_s = 0.5 cm and a thermal conductivity of 130 W/m K, it generates a quantity of heat Q = 300 W. The heat is mainly evacuated by conduction through the solid and then dissipated by convection of the cooling fluid in the $10 \times 46 \times 7.5\,cm^3$ parallelepipedic channel where the whole unit (heat sink + electronic component) is mounted.

2.2. Governing equations

The heat of the heat sink is transferred from its walls to flowing fluid. To simplify the analysis, the following assumptions have been made:

- The heat transfer and fluid flow in the heat sink are three-dimensional flows and in steady-state;
- Fluid flow is incompressible, single-phase and laminar;
- Negligible heat transfer by radiation.
- The thermophysical properties of nanofluids are constant, with the exception of the variation in density of buoyancy forces which is determined by the Boussinesq approximation.
- Nanoparticles are assumed to be uniform in shape and size, spherical and in a state of thermal equilibrium with the base fluid.
- Viscous dissipation is negligible.

Based on these assumptions, 3D steady governing equations of mass, momentum and energy conservation for fluid and the solid region in the heat sink can be written as:

- **Continuity equation:**

$$\frac{\partial u}{\partial x} + \frac{\partial v}{\partial y} + \frac{\partial w}{\partial z} = 0 \tag{1}$$

- **x-Momentum equation:**

$$\rho_o\left[\frac{\partial(uu)}{\partial x} + \frac{\partial(vu)}{\partial y} + \frac{\partial(wu)}{\partial z}\right] = -\frac{\partial p}{\partial x} + \frac{\partial}{\partial x}\left[\mu\frac{\partial u}{\partial x}\right] + \frac{\partial}{\partial y}\left[\mu\frac{\partial u}{\partial y}\right] + \frac{\partial}{\partial z}\left[\mu\frac{\partial u}{\partial z}\right] \tag{2}$$

- **y-Momentum equation:**

$$\rho_o\left[\frac{\partial(uv)}{\partial x} + \frac{\partial(vv)}{\partial y} + \frac{\partial(wv)}{\partial z}\right] = -\frac{\partial p}{\partial y} + \frac{\partial}{\partial x}\left[\mu\frac{\partial v}{\partial x}\right] + \frac{\partial}{\partial y}\left[\mu\frac{\partial v}{\partial y}\right] + \frac{\partial}{\partial z}\left[\mu\frac{\partial v}{\partial z}\right] \tag{3}$$

- **z-Momentum equation:**

$$\rho_o\left[\frac{\partial(uw)}{\partial x} + \frac{\partial(vw)}{\partial y} + \frac{\partial(ww)}{\partial z}\right] = -\frac{\partial p}{\partial z} + \frac{\partial}{\partial x}\left[\mu\frac{\partial w}{\partial x}\right] + \frac{\partial}{\partial y}\left[\mu\frac{\partial w}{\partial y}\right] + \frac{\partial}{\partial z}\left[\mu\frac{\partial w}{\partial z}\right] + g\beta(T - T_0) \tag{4}$$

- **Energy equation**
  – Fluid Side

$$\rho_o C_p\left[u\frac{\partial T}{\partial x} + v\frac{\partial T}{\partial y} + w\frac{\partial T}{\partial z}\right] = \frac{\partial}{\partial x}\left[k_f\frac{\partial T}{\partial x}\right] + \frac{\partial}{\partial y}\left[k_f\frac{\partial T}{\partial y}\right] + \frac{\partial}{\partial z}\left[k_f\frac{\partial T}{\partial z}\right] \tag{5}$$

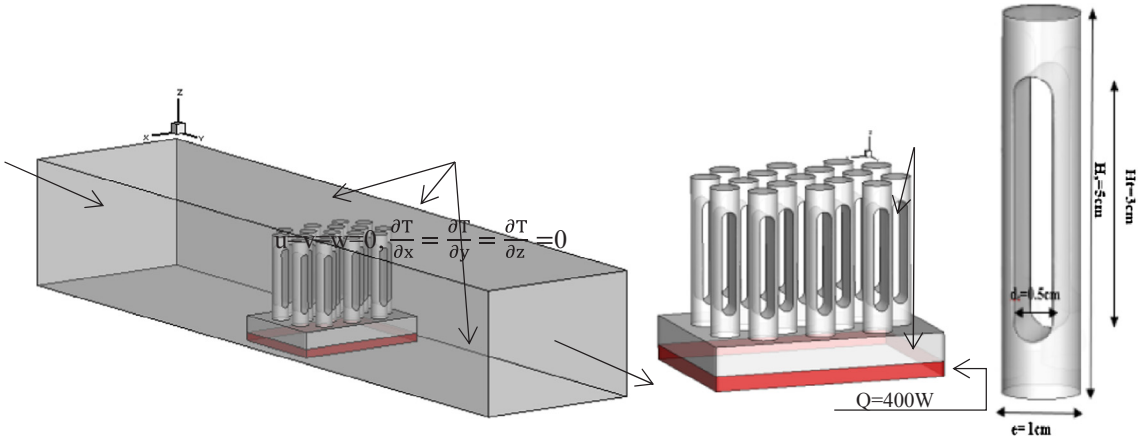

Fig. 1. Designed geometry and dimensions of pin-fin heat sink.

– Solid Side

$$k_S\left(\frac{\partial^2 T}{\partial x^2}+\frac{\partial^2 T}{\partial y^2}+\frac{\partial^2 T}{\partial z^2}\right)+\dot{q_S}=0 \quad (6)$$

where k_f and k_S are the heat sink thermal conductivity, respectively, of the fluid and the solid, $\dot{q_S}$ is the heat generated per unit volume;

2.3. Boundary conditions

The boundary conditions used to complete the model are:

- At the channel inlet: Inlet flow condition (velocity-inlet)

$$u = w = 0, \quad v = u_0, \quad T = T_o = 293.16 \ K$$

The velocity inlet is obtained from theReynolds number.

$$u_0 = \frac{Re\cdot\mu}{\rho\cdot D_h} \quad (7)$$

where D_h is hydraulic diameter.

- At the channel outlet: Outlet condition (pressure outlet)

$$\frac{\partial u}{\partial x}=\frac{\partial v}{\partial x}=\frac{\partial w}{\partial x}=\frac{\partial T}{\partial x}=0, \quad P = P_{atm} \quad (8)$$

- The no-slip adiabatic boundary conditions are applied at all walls of the channel

$$\frac{\partial T}{\partial x}=\frac{\partial T}{\partial y}=\frac{\partial T}{\partial z}=0, \quad u = v = w = 0 \quad (9)$$

- The heat flux between the interface of the fluid and the solid walls is coupled. Hence, the continuity between the interface of the solid and the fluid is given as:

$$k_S\frac{\partial T}{\partial n}\bigg|_{wall} = k_f\frac{\partial T}{\partial n}\bigg|_{wall} \quad (10)$$

- A heat source $\dot{q_s}$ is generated inside of the electronic component.

$$\dot{q}_s=\frac{Q}{V}, \quad Q = 300W, \quad V = 8 \ cm \times 6 \ cm \times 0.5 \ cm = 24 \ cm^3$$

2.4. Thermophysical properties of nanofluids

In this article, if a nanofluid is used as a coolant, the thermophysical properties in the governing equations are replaced by those of nanofluid. Three types of nanofluids were examined mathematically: TiO_2, Al_2O_3, Cu Nanoparticles dispersed in water. The thermophysical properties of the water and nanoparticles used in the calculations are given in Table 1.

The nanoparticles with 2%, 4%, 6%, 6%, 8% and 10% of the volume fraction were used for the thermophysical properties of the nanofluids, which were used in this calculation. The density, viscosity, specific heat and thermal conductivity of nanofluid were determined using the following equations: (11) to (15):

- Density:

$$\rho_{nf} = (1-\varphi)\rho_{np} + \varphi\rho_f \quad (11)$$

where ρ_{nf}, ρ_{np}, and ρ_f are densities of the nanofluid, nanoparticle, andbase fluid, respectively.

- Specific heat:

$$(\rho c_p)_{nf} = (1-\varphi)(\rho c_p)_f + \varphi(\rho c_p)_{np} \quad (12)$$

where c_p is the specific heat, φ is the particle volume fraction, and subscript nf, np and f are nanofluid, nanoparticles and base fluid, respectively.

- The Hamilton and Crosser model [45] is used to calculate the thermal conductivity (k) of nanofluids which are expressed as follows:

$$k_{nf} = k_f\left[\frac{k_{np}+2k_f-2(k_f-k_{np})\varphi}{k_{np}+2k_f+2(k_f-k_{np})\varphi}\right] \quad (13)$$

- The Brinkman relation [46] is used to calculate effective dynamic viscosity (μ):

$$\mu_{nf} = \frac{\mu_f}{(1-\varphi)^{2.5}} \quad (14)$$

- The coefficient of thermal expansion of the nanofluid β_{nf} can be determined by the equation:

$$\beta_{nf} = (1-\varphi)\beta_f + \varphi\beta_{np} \quad (15)$$

2.5. Numerical procedures

The geometry is created and meshed using the commercial software GAMBIT. The mesh file is exported to CFD software package, FLUENT 6.3.26, which employs a finite volume method for solves the integral equations for mass, momentum and fluid conservation and the solid phase energy equations. The detail of this method is explained by Patankar [47]. The 3D doubleprecision pressure based solver is selected with a standard SIMPLEalgorithm as its pressure–velocity coupling method. A body force weighted scheme is used for the pressure equation while apower law scheme is used to discretise thecombined convection and diffusion terms in the momentum andenergy equations. This is an iterative solution procedure initiated by pressure prediction fluid field. The continuity equation is efficient to be used to calculate the pressure drop. The solution is considered sufficiently convergent when the normalized residual value of 10^{-3} for momentum and mass and 10^{-6} for energy equations.

2.6. Grid independence test

Different non-uniform mesh sizes are taken into account in this study, in order to examine the independence of the mesh size and to ensure the accuracy and reliability of the numerical solution before performing the calculations, triangularand hexagonal cells were used to mesh the geometry, as shown in Fig. 2. The grid independence was verified for pure water using different mesh sizes, as shown in Fig. 3, all of which were tightened near the walls to capture the effects of the boundary layer in these regions.

The average Nusselt number was determined for all mesh faces at Reynolds number $Re = 400$.

From Fig. 3, we see that the difference between the average Nusselt values for the last three mesh sizes is slightly different, the average Nusselt number becomes insensitive to the number of nodes in the 1.96254×10^6 grid. Therefore, we have chosen 1.96254×10^6 nodes for all our calculations, in order to obtain qualitative results with a minimum of computation time.

Table 1
Thermophysical properties of nanoparticles and water.

Properties	Water	TiO_2	Al_2O_3	Cu
P (kg/m^3)	998.2	4250	3970	8933
Cp (J/kg k)	4179	686.2	765	385
β (K^{-1})	21×10^{-5}	0.9×10^{-5}	0.85×10^{-5}	1.67×10^{-5}
k (W/m k)	0.61	8.9538	40	400

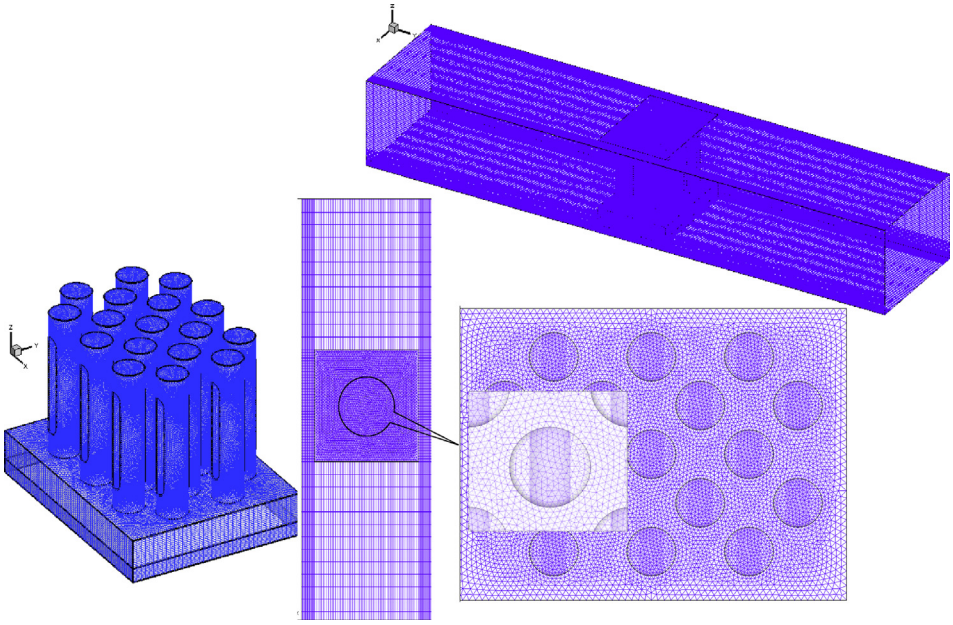

Fig. 2. Configuration Mesh.

2.7. Data analysis

Major results such as total heat transfer rate, average outlet temperature, average bulk temperature, pressure drop and mass flow rate were obtained from the FLUENT outlet results. The Nusselt number, friction factor and pumping power of the pin fins array were calculated using the thermal transfer relationships.

The total heat removed by the flowing fluid inside the channelcan be calculated as;

$$Q = \dot{m} \cdot c_p \cdot (\overline{T}_{out} - T_0)$$

where $\dot{m}$ is the mass flow rate, $c_p$is the specific heat, T_0 and $\overline{T}_{out}$arethe inlet and outlet flowing fluid temperatures.

The average heat transfer coefficient is used to investigate theheat transfer. It is defined by,

$$\overline{h} = \frac{Q}{A.\,(\overline{T}_w - \overline{T}_{m)}}$$

- $\overline{T}_w$wall mean temperature
- $\overline{T}_m$ bulk mean temperature

The Nusselt number gives the ratio of actual heat transferred of the pin-fins array by themoving fluid to the equivalent heat transfer that would occur by conduction. The Nusseltnumber was defined as:

$$\overline{Nu} = \frac{\overline{h} \cdot D_h}{k_{nf}}$$

In order to estimate the improvement of the heat transfer in nanofluids compared to the pure fluid, we define percentageenhancement of the Nusselt number of nanofluidas follows:

$$\text{Enhancement } \overline{Nu}\% = \frac{Nu_{nf} - Nu_f}{Nu_{nf}} \times 100$$

The pressure drag coefficient is calculated as follows:

$$f = \frac{\Delta p}{0.5.\,\rho.\,u_0^2} \cdot \frac{D_h}{L} \quad (16)$$

where Δp is the pressure drop across the heat sink

$$\Delta p = p_{inlet} - p_{out}$$

The Pumping power (PP) is calculated as follows:

Number of nods	$\overline{Nu}$
382585	56,8887
505570	55,65679
1,15475x10^6	54,53475
1,35636 x10^6	53,61062
1,49758 x10^6	52,72412
1,70706 x10^6	52,01875
1,87568 x10^6	51,42647
1,96254 x10^6	**51,11596**
2,25708 x10^6	51,01245
2,4062 x10^6	51,00873

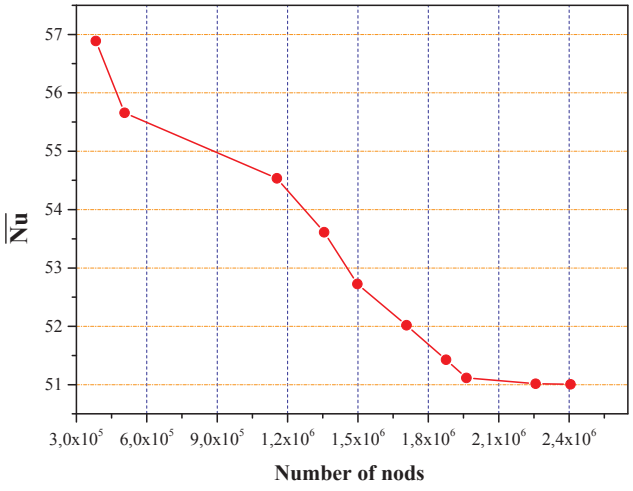

Fig. 3. Variation of the number of Nusselt as a function of the number of mesh nodes for *Re* = 400.

$PP = \Delta P \cdot \dot{V}$

$\dot{V}$ the volume flow rate

3. Results and discussion

3.1. Temperature field and flow characteristics in heat sink

Fig. 4 illustrates the temperature distribution through a temperature contour in the pin fin heat sink for the three types of naofluids studied and for the Reynolds number Re = 400 and the volumetric fraction φ = 10%. It can be seen that the average temperatures of the solid pin fins are high and that their internal temperature is not uniform. It should also be noted that the maximum temperature is recorded at the base of the fins and decreases from the base to the ends as the fin takes heat from the heated base plate which has in turn been heated by the heat produced by the electronic component.

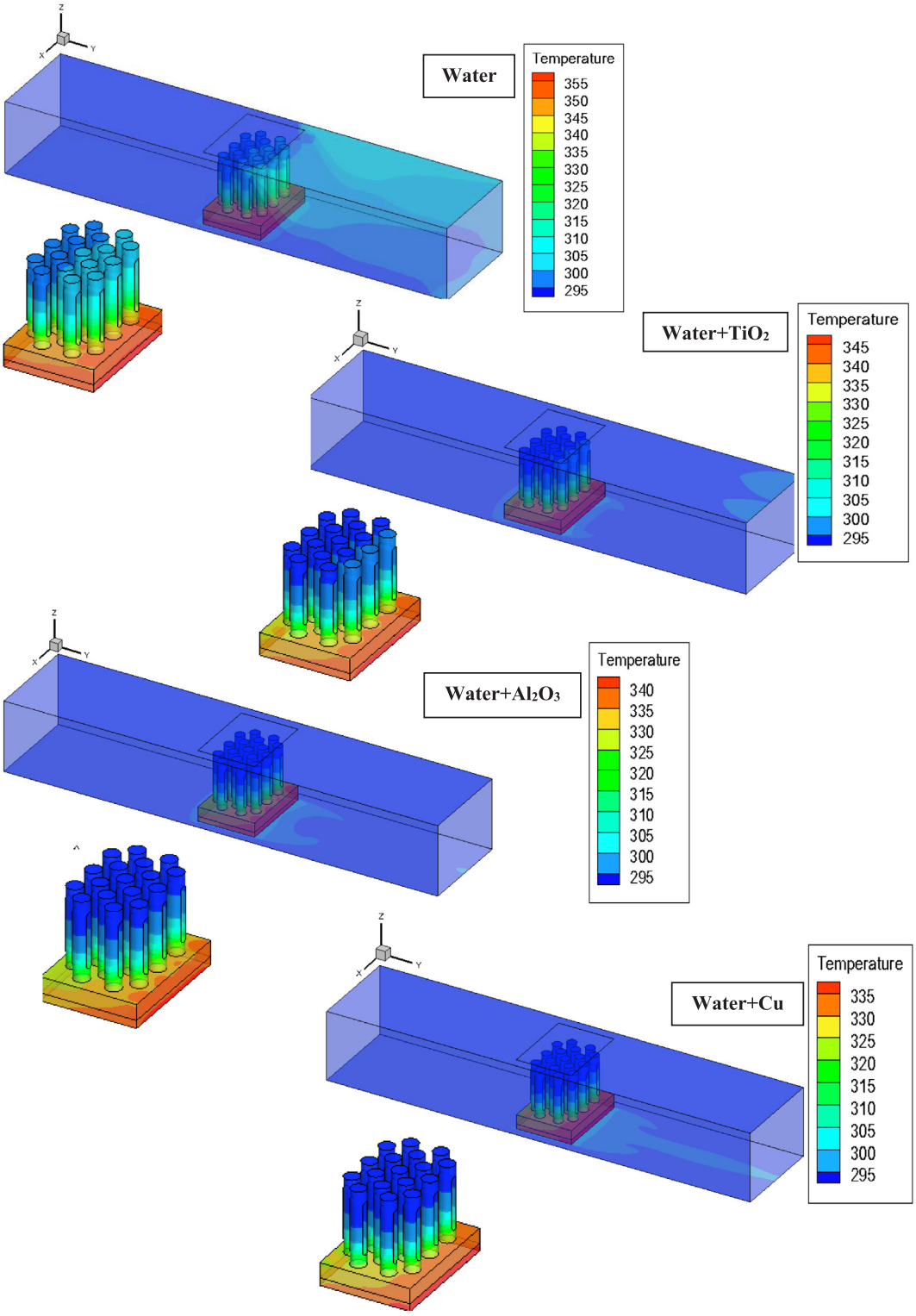

Fig. 4. Contours of temperature in the channel and in the solid heat sink for φ = 10%, Re = 400.

This figure shows that the use of nanofluid as a coolant instead of pure water improves the heat transfer process by reducing the temperature of the pin fins, the Cu-water nanofluid gives the low wall temperature and therefore a high heat transfer rate compared to TiO_2-water and Al_2O_3-water nanofluid, on the other hand, pure water gives a higher pin temperature and therefore a lower heat transfer.

Also we can see that fins plays an important role in increasing heat transfer by increasing the heat transfer surface and creating the mixture in flow

Fig. 5 shows the contours and velocity vectors as well as the pathlines of the nanofluid Cu + water in the plane x = 0.03 m for a Reynolds number *Re* = 400 and for a different volumetric fraction. The graph clearly shows that the dynamic fields undergo a uniform velocity profile at the input of the heat sink. The direction of the velocity vector changes as the nanofluid particles approach the fin body and move above it. After passing through the body at a short distance, the velocity vectors return to their original direction, showing that the flow is laminar. We can also see that the velocity profile around the fins has the same tendency for different fractions. The flow velocity within the perforation and in the fin space reaches maximum values due to the reduction of the perforation section and fin space, the acceleration of the hot nanofluid promotes thermal transfer by convection. It is clearly observable that the flow velocity decreases as the volume fractions increase, which justifies the decrease in heat exchange with the increase

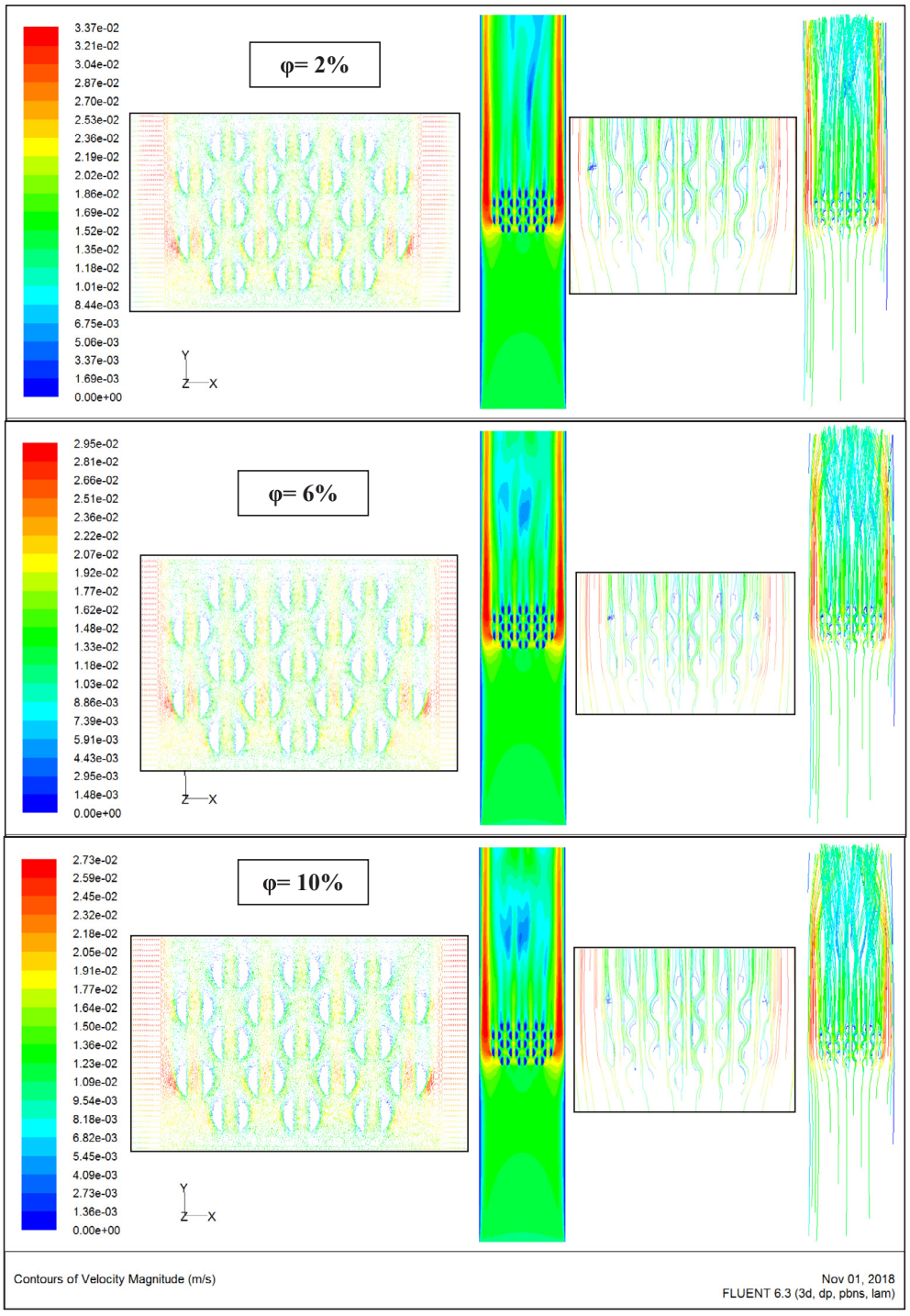

Fig. 5. Contours of velocity and pathlines of nanofluid (water + Cu) in plan z = 0.03 m, *Re* = 400.

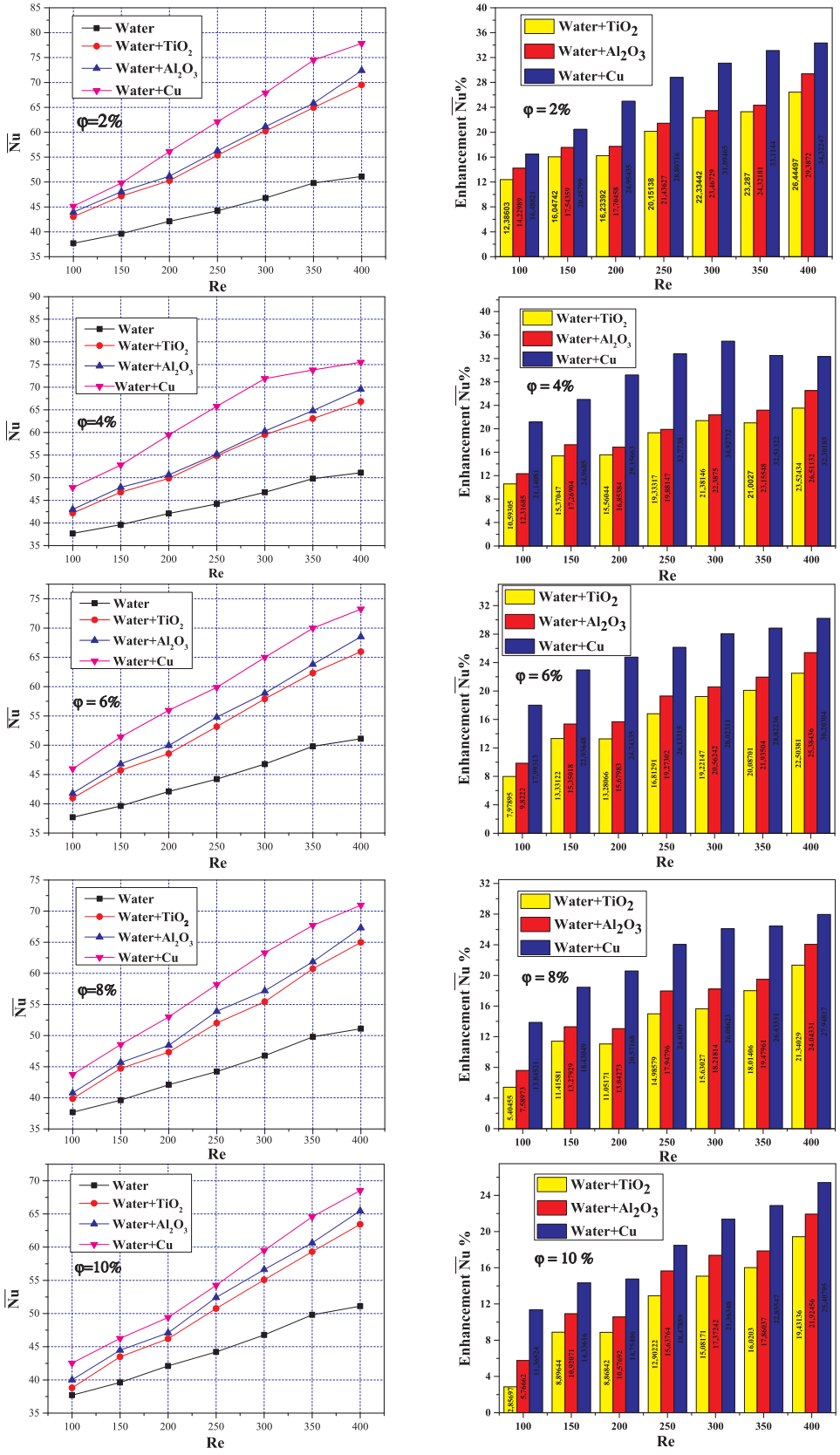

Fig. 6. Variation of the mean Nusselt number and its enhancement according to Reynolds number andvolumetric concentration.

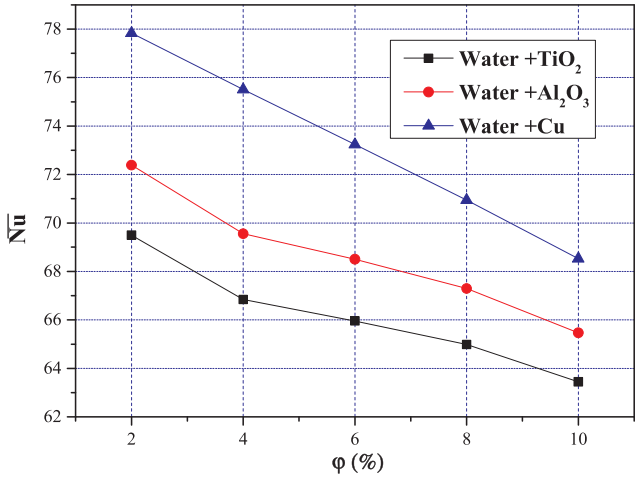

Fig. 7. Variation of the mean Nusselt number according to volumetric concentration, *Re* = 400.

of φ.

This figure also shows the flow pathlines for the different volumetric fractions. For all values of φ, the flow is known as crawling. Viscosity forces being dominant, the fluid remains attached to the fins without any separation. The flow is symmetrical for each fin column with respect to its central axis and also between the upstream and downstream of the fin.

3.2. Variation of the Nusselt number

Fig. 6 shows the variation in the average of Nusselt number and its percentage enhancement as a function of the Reynolds number for the three suspensions considered (TiO_2, Al_2O_3 and Cu). The results are presented for nanoparticle volume fractions of 2%, 4%, 6%, 8%, 10%. We can note that the Nusselt number and therefore the heat transfer increases with the increase in the Reynolds number.

Table 1 shows that TiO_2 has the lowest thermal conductivity value compared to other nanoparticles, therefore, it has the lowest values of the Nusselt number. Cu and Al_2O_3, on the other hand, have the highest values. In addition, the Nusselt number for Al_2O_3 is lower than that of Cu. The heat transfer rate is maximum for copper (Cu) compared to Al_2O_3 and TiO_2. This result is due to the thermophysical properties of copper. Copper nanoparticles allow for better heat exchange. This exchange is favorated by a higher conductivity to evacuate heat, a lower thermal capacity to reduce storage and a higher density to promote convection (Archimedes' force).

This figure also shows that all the nanofluids used offer a more interesting heat transfer than in the case of the base fluid. This implies that whatever the type of nanofluid used as a heat transfer fluid, it contributes to improving heat transfer.

We observe that the Nusselt number enhancement increases with the Reynolds number and decreases with the volume concentration of nanofluid. The enhancement in the Nusselt number for the nanofluid Cu + water is higher than for Al_2O_3 + water and TiO_2 + water records the lowest values.

For example, the heat transfer enhancementvalues for φ = 2% and $100 \leq Re \leq 400$ are 12.36% to 26.44% for the nanofluid TiO_2 + water, 14.22% to 29.38% for the nanofluid Al_2O_3 + water and 16.48% to 34.32% for the nanofluid Cu + water.

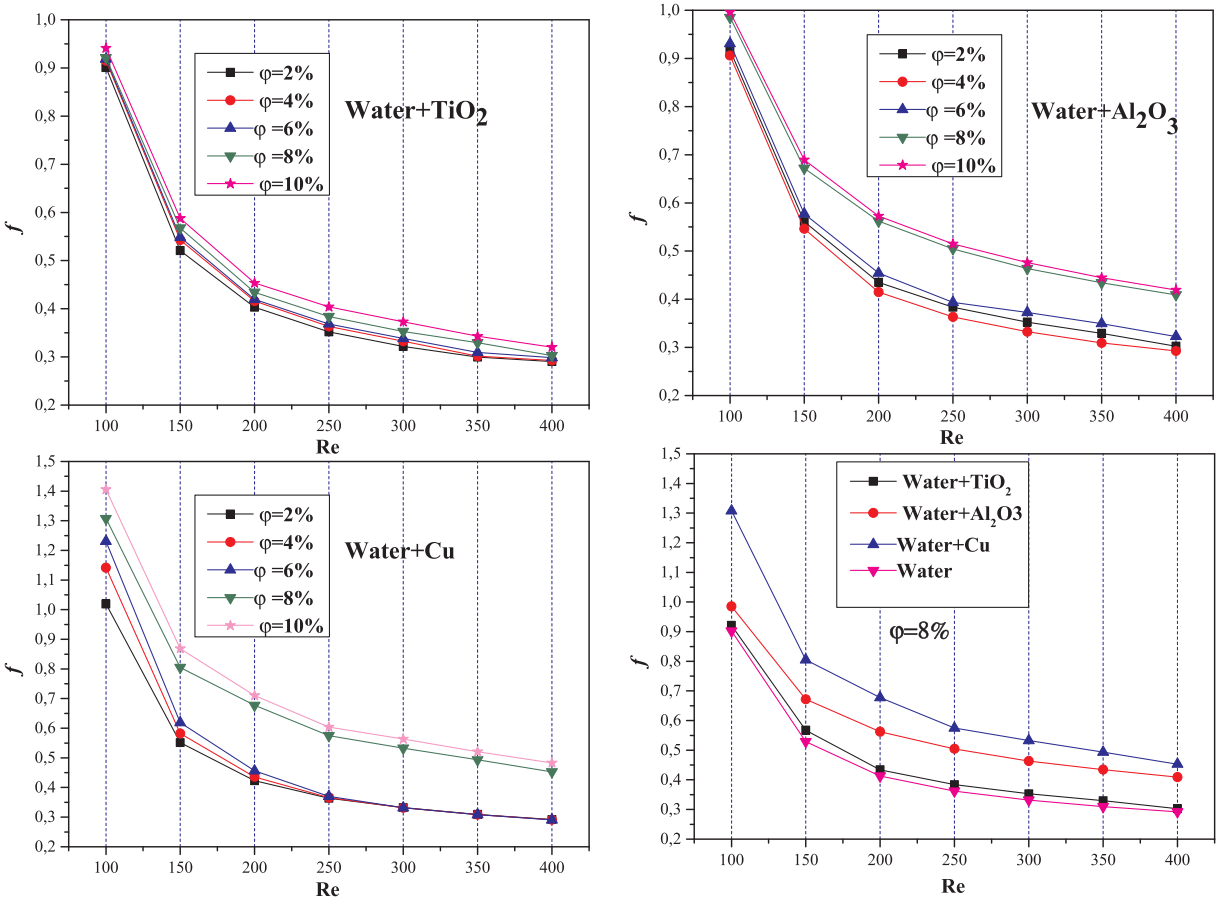

Fig. 8. Variation of the friction factor according to Reynolds number andvolumetric concentration.

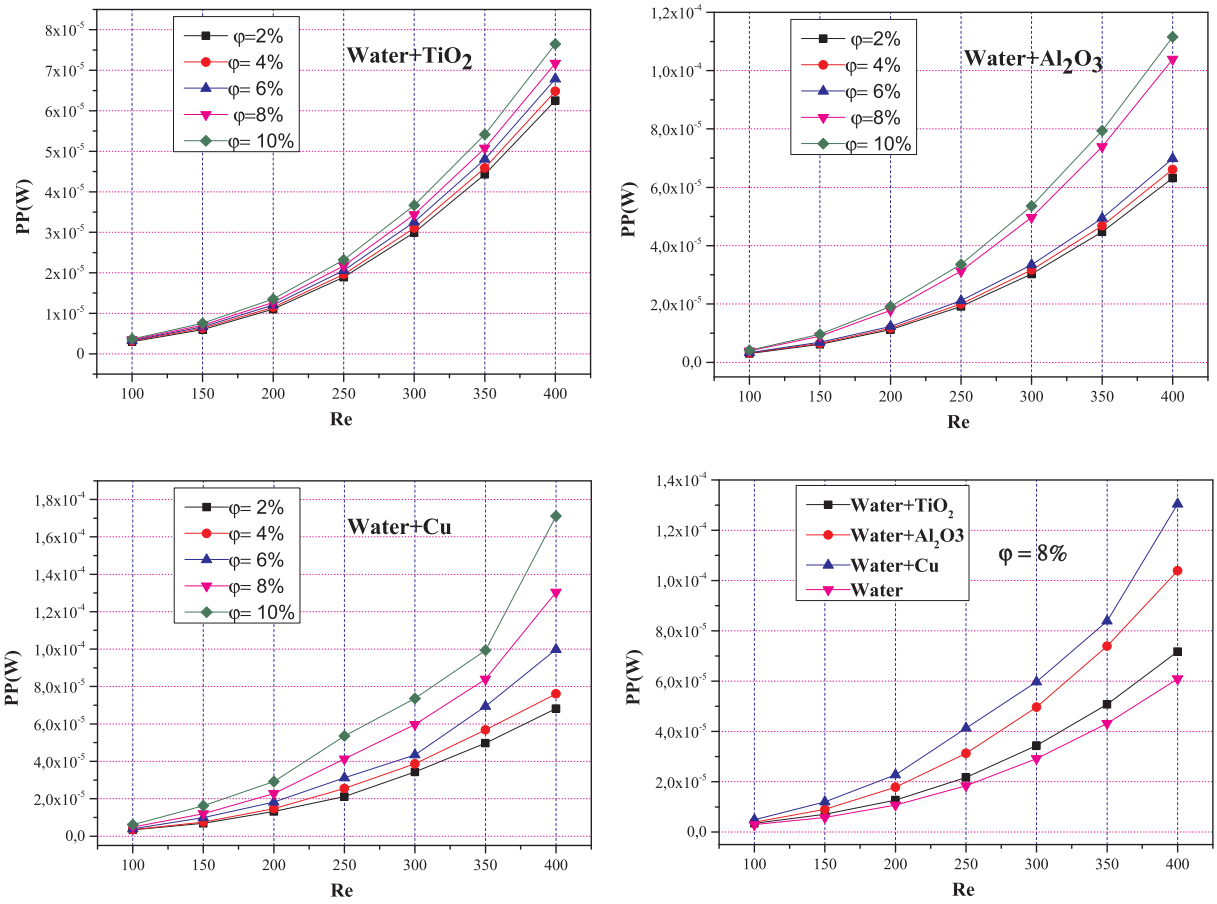

Fig. 9. Variation of the pumping power according to Reynolds number andvolumetric concentration.

The variation in the average number of Nusselt as a function of the volumetric fraction of the nanoparticles used (Cu, Al_2O_3 and TiO_2) is shown in Fig. 7. Results are obtained for a Reynolds number Re = 400, it should be noted that heat transfer decreases with increasing volumetric fraction and thermal conductivity of nanoparticles.

Contrary to what many authors have obtained, we have shown in this work that in our configuration, heat transfer is higher in nanofluids with a low volumetric fraction. The Nusselt number of nanofluids decreases with the increase in the volumetric fraction of nanoparticles.

It is true that the addition of nanoparticles of TiO_2, Al_2O_3 and Cu in pure water increases its thermal conductivity and thus improves the conduction heat transfer in nanofluids compared to the conduction heat transfer in the base fluid.

But on the other hand, we have found that the suspension of nanoparticles in pure water with a high volume fraction causes an increase in dynamic viscosity with a decrease in the thermal capacity of nanofluids, which leads to a decrease in flow velocity and thermal convective transfer.

3.3. The friction factor

Fig. 8 shows the variant of the friction factor in relation to the Reynolds number for various volume fractions of nanofluid in the heat sink. As shown in this figure, the friction factor of nanofluid decreases with the increase in *Re*, which is similar to that of pure water, and the increase in the friction factor with the addition of nanoparticles is due to an increase in pressure drop.

The friction factor for pure water and TiO_2 + water nanofluid is almost the same. The nanofluid Al_2O_3 seems to give a slight increase in the friction factor and Cu + water gives a maximum value.

3.4. The pumping power

In addition, Fig. 9 also shows the variation in pumping power as a function of the Reynolds number of pure water and nanofluids for different concentrations. It can be seen that as the Reynolds number increases, a higher pumping power is required for different coolants. This figure also shows that pumping power increases with the increase in Reynolds number for different coolants. This is due to the fact that as the inlet velocity increases, the pressure drop is increased, so more power is required for pumping. In addition, it is obvious that the heat sink with nanofluid has the highest pumping power compared to pure water. With regard to the effect of nanoparticle concentration, it can be seen that the addition of nanoparticles increases pumping power.

4. Conclusion

The mixed convective heat transfer on nanofluids in a three-dimensional heatsink with perforated circular fins is numerically studied using the finite volume method. TiO_2, Al_2O_3 and Cu are used as nanoparticles. The selected volumetric concentration of nanofluids was chosen in the range (2–10)%. The Reynolds number has changed between 100 and 400. The effects of the volume fraction and Reynolds number are carefully studied on the thermal and hydraulic behaviour of nanofluids. The results show that with the increase in the volume fraction, the Nusselt number and its overall enhancement decrease.

In addition, with the increase in the Reynolds number, the Nusselt number and overall heat transfer increase. It has been found that TiO_2 has the lowest value of the Nusselt number. Cu and Al_2O_3, have the highest values. In addition, the Nusselt number for Al_2O_3 is lower than that of Cu. The thermal transfer rate is maximum for copper (Cu) compared to Al_2O_3 and TiO_2. Finally, we noted that the friction factor

and pumping power of nanofluids increase with the increase in Reynolds number, which is similar to that of pure water, and they increase with the addition of nanoparticles. It can be seen that the addition of nanoparticles increases pumping power.

References

[1] E.A.M. Elshafei, Natural convection heat transfer from a heat sink with hollow/perforated circular pin fins, Energy 35 (2010) 2870–2877.
[2] O.N. Sara, T. Pekdemir, S. Yapici, M. Yilmaz, Heat transfer enhancement in a channel flow with perforated rectangularblocks, Int. J. Heat Fluid Flow 22 (2001) 509–518.
[3] M.R. Shaeri, M. Yaghoubi, Thermal enhancement from heat sinks by using perforated fins, Energy Convers. Manage. 50 (2009) 1264–1270.
[4] C. Manikandan, S. Pachaiyappan, Transient thermal simulation of perforated drop-shaped pin fin array in staggered arrangement, Int. J. Innovative Res. Sci. Eng. Technol. 5 (2) (2016) 2193–2202.
[5] F.Z. Bakhti, M. Si-Ameur, Numerical study of cooling enhancement:heat sink with hollow perforated ellipticpin fins, Comput. Therm. Sci. 8 (5) (2016) 409–428.
[6] H. Masuda, A. Ebata, K. Teramae, N. Hishinuma, Alteration of thermal conductivity and viscosity of liquid by dispersing ultra-fine particles(dispersion of Al2O3, SiO2 and TiO2 ultra-fine particles), Netsu Bussei (Jpn.) 7 (4) (1993) 227–233.
[7] Stephen U.S. Choi, Jeffrey A. Eastman, Enhancing thermal conductivity of fluids with nanoparticle, ASME Int. Mech. Eng. Congr. Exposition (1995).
[8] S. Lee, S.U.S. Choi, S. Li, J.A. Eastman, Measuring thermal conductivity of fluids-containing oxidenanoparticles, ASME J. Heat Transfer 121 (1999) 280–289.
[9] B.X. Wang, L.P. Zhou, X.F. Peng, A fractal model for predicting the effectivethermal conductivity of liquid with suspension of nanoparticles, Int. J. Heat Mass Transfer 46 (2003) 2665–2672.
[10] J. Koo, C. Kleinstreuer, A new thermal conductivity model for nanofluids, J. Nanopart. 6 (2004) 577–588.
[11] W. Duangthongsuk, S. Wongwises, Heat transfer enhancement and pressure-dropcharacteristics of TiO_2–water nanofluid in a double-tube counter flowheat exchanger, Int. J. Heat Mass Transfer 52 (2009) 2059–2067.
[12] W. Duangthongsuk, S. Wongwises, Measurement of temperature-dependentthermal conductivity and viscosity of TiO_2–water nanofluids, Exp. Therm. Fluid Sci. 33 (2009) 706–714.
[13] W. Duangthongsuk, S. Wongwises, An experimental study on the heat transfer-performance and pressure drop of TiO_2–water nanofluids flowing under turbulent flow regime, Int. J. Heat Mass Transfer 52 (2010) 334–344.
[14] W. Duangthongsuk, S. Wongwises, A dispersion model for predicting the heat-transfer performance of TiO_2–water nanofluids under a laminar flow regime, Int. J. Heat Mass Transfer 55 (2012) 3138–3146.
[15] W. Duangthongsuk, A.S. Dalkilic, S. Wongwises, Convective heat transfer ofAl_2O_3–water nanofluids in a microchannel heat sink, Curr. Nanosci. 8 (2012) 317–322.
[16] S.P. Jang, S. Choi, Cooling performance of a microchannel heat sink with nano-fluids, Appl. Therm. Eng. 26 (2006) 2457–2463.
[17] J. Li, C. Kleinstreuer, Thermal performance of nanofluid flow in microchannels, Int. J. Heat Fluid Flow 29 (2008) 1221–1232.
[18] Seyed Ebrahim Ghasemi, A.A. Ranjbar, M.J. Hosseini, Numerical study on effect of CuO-water nanofluid on cooling performance of two different cross-sectional heat sinks, Adv. Powder Technol. 28 (2017) 1495–1504.
[19] M. Ghazvini, H. Shokouhmand, Investigation of a nanofluid-cooled micro-channelheat sink using fin and porous media approaches, Energy Convers. Manage. 50 (2009) 2373–2380.
[20] P. Selvakumar, S. Suresh, Convective performance of CuO/water nanofluid in an electronic heat sink, Exp. Thermal Fluid Sci. 40 (2012) 57–63.
[21] H.A. Mohammed, P. Gunnasegaran, N.H. Shuaib, Heat transfer in rectangular microchannel sheat sink using nanofluids, Int. Commun. Heat Mass Transfer 37 (2010) 1496–1503.
[22] C.J. Ho, L.C. Wei, Z.W. Li, An experimental investigation of forced con-vectivecooling performance of a microchannel heat sink with Al_2O_3/water nano-fluid, Appl. Therm. Eng. 30 (2010) 96–103.
[23] M. Kalteh, A. Abbassi, M.S. Avval, A. Frijns, A. Darhuber, J. Harting, Experimental and numerical investigation of nanofluid forced convectioninside a wide micro-channel heat sink, Appl. Therm. Eng. 36 (2012) 260–268.
[24] C.J. Ho, W.C. Chen, An experimental study on thermal performance of Al_2O_3/wa-ternanofluid in a minichannel heat sink, Appl. Therm. Eng. 50 (2013) 516–522.
[25] C. Anbumeenakshi, M.R. Thansekhar, On the effectiveness of a nanofluid cool-edmicrochannel heat sink under non-uniform heating condition, Appl. Therm. Eng. 113 (2017) 1437–1443.
[26] M.R. Sohel, S.S. Khaleduzzaman, R. Saidur, A. Hepbasli, M.F.M. Sabri, I.M. Mahbubul, An experimental investigation of heat transfer enhancement of aminichannel heat sink using Al2O3–H2O nanofluid, Int. J. Heat Mass Transfer 74 (2014) 164–172.
[27] C.J. Ho, Y.N. Chung, C.-M. Lai, Thermal performance of Al_2O_3/water nanofluid ina natural circulation loop with a mini-channel heat sink and heat source, Energy Convers. Manage. 87 (2014) 848–858.
[28] Seyed Ziaedin Miry, Sina Lohrasbi, Hesam Irani, Mehdi Ashjaee, Davood Domiri Ganji, Thermal energy absorption in a heat sink with elliptical cross section and tangential impinging inlet flow of nanofluid, Exp. Thermal Fluid Sci. 89 (2017) 50–61.
[29] Muhammad Saeed, Man-Hoe Kim, Heat transfer enhancement using nanofluids (Al_2 $_O3$–$_H2O$) in mini-channel heatsinks, Int. J. Heat Mass Transfer 120 (2018) 671–682.
[30] H.A. Mohammed, P. Gunnasegaran, N.H. Shuaib, The impact of variousnanofluid types on triangular microchannel heat sink cooling performance, Int. Commun. Heat Mass Transfer 38 (2011) 767–773.
[31] T.C. Hung, W.M. Yan, X.D. Wang, C.Y. Chang, Heat transfer enhancement in mi-crochannelheat sinks using nanofluids, Int. J. Heat Mass Transfer 55 (2012) 2559–2570.
[32] A. Ijam, R. Saidur, P. Ganesan, Cooling of minichannel heat sink usingnanofluids, Int. Commun. Heat Mass Transfer 39 (2012) 1188–1194.
[33] A. Ijam, R. Saidur, Nanofluid as a coolant for electronic devices (cooling ofelec-tronic devices), Appl. Therm. Eng. 32 (2012) 76–82.
[34] E. Manay, B. Sahin, M. Yilmaz, K. Gelis, Thermal performance analysis of nanofluids in microchannel heat sinks, World Acad. Sci. Eng. Technol. 67 (2012) 100–105.
[35] A.K.O. Albdoor, Numerical investigation of laminar nanofluid flow in micro chan-nelheat sinks, Int. J. Mech. Eng. Technol. (IJMET) 5 (2014) 86–96.
[36] E.M. Tokit, H.A. Mohammed, M.Z. Yusoff, Thermal performance of optimize-dinterrupter microchannel heat sink (IMCHS) using nanofluids, Int. Commun. Heat Mass Transfer 39 (2012) 1595–1604.
[37] S.M.H. Hashemi, S.A. Fazile, H. Zirakzadeh, M. Ashjaee, Study of heat transfer-enhancement in a nanofluid-cooled miniature heat sink, Int. Commun. Heat Mass Transfer 39 (2012) 877–884.
[38] P. Naphon, L. Nakharintr, Heat transfer of nanofluid in the mini-rectangular fin heat sink, Int. Commun. Heat Mass Transfer 40 (2013) 25–31.
[39] Mushtaq Ismael Hasan, Investigation of flow and heat transfer characteristics in micro pin finheat sink with nanofluid, Appl. Thermal Eng. 63 (2014) 598–607.
[40] S.B. Abubakar, N.A.C. Sidi, Numerical prediction of laminar nanofluid flow in rectangular microchannel heat sink, J. Adv. Res. Fluid Mech. Therm. Sci. 7 (2015) 29–38.
[41] S.B. Abubakar, N.A.C. Sidik, A.S. Ahmad, The use of Fe_3O_4-H_2O_4 nanofluid forheat transfer enhancement in rectangular microchannel heat sink, J. Adv. Res. Fluid Mech. Therm. Sci. 23 (2016) 15–24.
[42] J. Zhang, Y. Diao, Y. Zhao, Y. Zhang, An experimental investigation of heat transfer enhancement in minichannel: combination of nanofluid and micro fin structure techniques, Exp. Therm Fluid Sci. 81 (2017) 12–32.
[43] W. Arshad, H.M. Ali, Experimental investigation of heat transfer and pressuredrop in a straight minichannel heat sink using TiO_2 nanofluid, Int. J. Heat Mass Transfer 110 (2017) 248–256.
[44] H. Salhi, M. Si-Ameur, D. Haddad, Numerical study of natural convection heat transfer performance in an inclined cavity with complex-wavy-wall: nanofluid and random temperature, Comput. Thermal Sci. 7 (1) (2015) 51–64.
[45] R. Hamilton, O. Crosser, Thermal conductivity of heterogeneous two-compo-nentsystems, Indust. Eng. Chem. Fundamentals 1 (3) (1962) 187–191.
[46] H. Brinkman, The viscosity of concentrated suspensions and solutions, J. Phys. 20 (1952) 571.
[47] S.V. Pantakar, Numerical Heat Transfer and Fluid Flow, Hemisphere Publishing Corp., 1980.